

Enhancement of Heat Transfer and Thermo-Hydraulic Performance Using Triangular Protrusions as Roughness Elements

A. Nagaraju*, Prof. B.Uma Maheswar Gowd**

*,**Department of Mechanical Engineering, Jawaharlal Nehru Technological University, Anantapur, Anantapuramu, 515 002, Andhra Pradesh, India

ABSTRACT

Solar heat has been thrust area of research to explore renewable energy utilisation for the past few decades. In solar air heaters artificial roughness is tried on the surface of the absorber plate by adding small roughness elements to enhance the heat transfer rate. In the present work triangular protrusion are provided to act as roughness elements over the surface of the aluminum absorber plate. The experimental study is carried out on the effect of change in apex angle of protrusions on the heat transfer rate by keeping the other design parameters unchanged. Maximum heat transfer rate and thermo-hydraulic performance between the range of apex angle 30° and 60° is studied. The Nusselt number is between 50 and 110, friction factor $4.5-6.7 \times 10^{-3}$, Stanton number is $6-14 \times 10^{-3}$. The heat transfer rate and thermo-hydraulic performance are observed to be maximum for 45° apex angle and least for the 60° plate.

Keywords – Friction Factor, Nusselt, Reynolds, Stanton Number, Thermo-Hydraulic performance.

I. INTRODUCTION

There are many ways for heating the air by using conventional sources of energy for industrial needs. Such resources account in many disadvantages like their scarcity, cost and emissions. So capturing solar energy is a solution to the man's quest for Non-Conventional source of energy. The solar thermal energy can be used to heat air. But such solar air heaters yield very low heat transfer rate and poor thermo-hydraulic performance because of the laminar sub-layer present at air and absorber plate interface. Various roughness elements like V-shaped rib by Momin et al., Wedge shaped rib by Bhagoria et al, Expanded Metal mesh by Saini and Saini, Angled circular rib by Gupta et al, small diameter protrusion wire by Prasad et al are studied experimentally Triangular protrusions have been used in the present work as roughness elements on the aluminum plate surface for the enhancement of heat transfer and thermo-hydraulic performance. The apex angle of the protrusions on plates is varied to find out how they affect heat transfer rate and thermo-hydraulic performance.

II. EXPERIMENTAL SET UP

An indoor setup consists of long duct $2400 \times 150 \times 15 \text{ mm}^3$ which is divided into three sections namely entry section of length 800mm which is more than the ASHRAE designated minimum length i.e., $5\sqrt{WH}$, Exit section of length 600mm which is more than ASHRAE standard value

of $2.5\sqrt{WH}$, the test section of length 1000mm where an aluminium absorber plate is placed. A schematic diagram is shown in Fig.1.

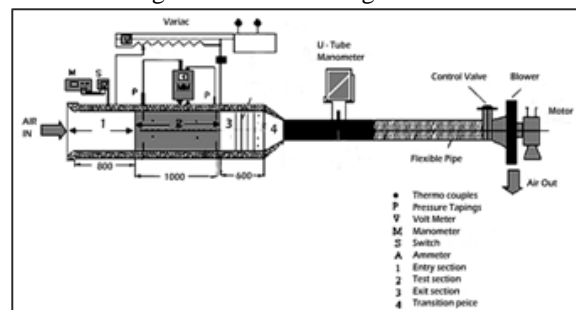


Fig 1. Line diagram of experimental set-up

III. FIGURES AND TABLES

To ensure a high-quality product, diagrams and lettering MUST be either computer-drafted or drawn using India ink.

Many researchers have reported the aspect ratio (W/H) to be between 8 and 15 may result in optimization of performance of the apparatus. The aspect ratio in the present study is chosen as 10. As the experiment is carried out in a laboratory an electric heater is chosen to simulate solar heating. The electric heater is made by fixing a Nichrome of wattage 1000 W/m^2 in zigzag pattern across the length of asbestos sheet. The ends of the Nichrome wire are connected to the terminals of a variac to maintain a constant electrical energy of 250W which is converted in to heat energy by the heater and radiated over to the absorber plate. The electric heater is

separated at a height above the absorber plate. 28SWG copper-constantan thermocouples are fixed across the length of the absorber plate as well as in the duct to measure the temperature of plate across its length and air flowing through the duct respectively.

The baffles are hanged in the exit section which helps in the mixing of air. A transition has been made that connects the wooden duct with the G.I. pipe to which centrifugal blower and bypass valve are attached. Another transition is used to join the other end of G.I. Pipe to the centrifugal blower. The centrifugal blower is coupled with a single phase induction motor which runs at 2800rpm. The blower creates vacuum in the duct to suck the atmospheric air and flow through it. A bypass valve is connected across the length of the G.I. Pipe to change the mass flow rate of air in the duct. The triangular protrusions on the surface of the absorber plate are machined over a CNC Milling centre. A view of the experimental setup is shown in Fig.2.



Fig.2 A view of Experimental set up

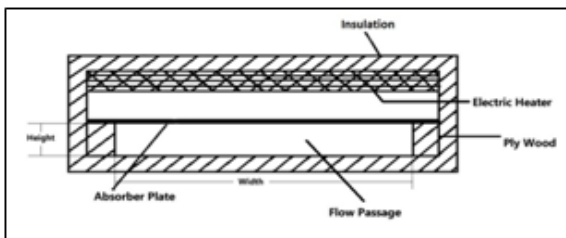


Fig.3. Cross-sectional view of the solar air heater

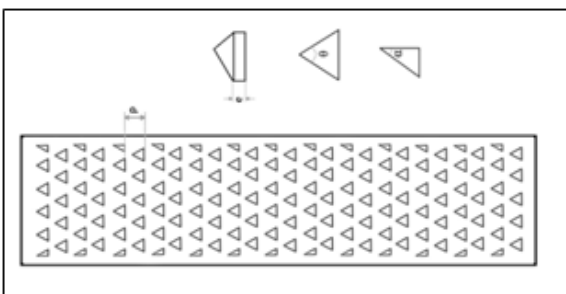


Fig.4. Schematic of Absorber Plate with Triangular protrusions

P Pitch of the roughness element
 e Height of roughness element
 α Angle of attack, θ Apex angle

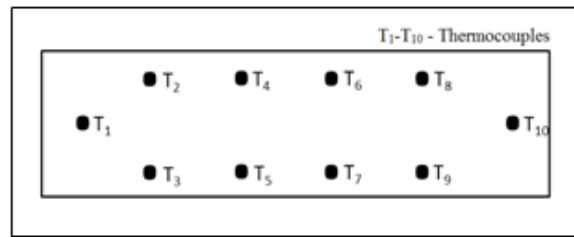


Fig 5. Line diagram of the thermocouples pattern over absorber plate

III EXPERIMENTATION

The set up is checked and instrumentation is fixed. The absorber plate is placed on the test section and the heater is placed above the absorber plate. The duct is then fully covered with thick glass wool insulation. The electric heater is connected to the variac. Copper-constantan thermocouples of gauge (28SWG) are used to measure the temperature of absorber plate and the air. Flow of air is controlled with the help of control valve. Initially the control valve is closed and switch on the heater. The plate is allowed to get heated and the blower is switch on. The temperature of the plate and air are maintained to assume steady state. The relevant data is collected. Later the absorber plate is replaced by another absorber plate with protrusions of different configurations and the experimentation is repeated.

IV. DATA REDUCTION

Average Temperature

The mean air temperature of Average flow temperature T_f is the measure values at the inlet and outlet of the test section. Thus,

$$T_f = (T_i + T_{oav})/2$$

The mean plate temperature T_{pav} is the average of the reading of all points located on the absorber plate.

Mass Flow Measurement

Mass flow rate is calculated using the equation.

$$m = C_d \times A_0 \times \left[\frac{2\rho\Delta P_0}{1 - \beta^4} \right]^{0.5}$$

Where

- M, Mass flow rate, kg/s
- C_d , Coefficient of discharge orifice
- A_0 , Area of orifice in m^2
- ρ , Density of air kg/m^3
- β , Ratio of diameter of orifice and pipe
- ΔP_0 , Pressure difference

Velocity Measurement

$$V = \frac{m}{\rho W H}$$

Where,

- ρ = density of air, Kg/m^3
- W = width of duct, m

H = height of duct, m

Reynolds Number

$$Re = \frac{VD_h}{\nu}$$

Where,

$$D_h = \text{Hydraulic diameter} = \frac{4WH}{2(W + H)}$$

ν = kinematic viscosity, m²/s

Heat Transfer Coefficient

Value of heat transfer coefficient between the absorber plate and fluid is given by the equation.

$$m C_p [t_o - t_i] = h A_p [t_p - t_f]$$

Where,

C_p = specific heat of air, J/Kg K

A_p = area of absorber plate, m²

Nusselt Number

$$Nu = \frac{hD_h}{K} \text{ Where}$$

K=thermal conductivity of air, W/m K

V. VALIDATION TEST

The values of Nusselt Number and friction factor determined from experimental data for smooth duct have been compared with the values obtained from modified Dittus – Boelter equation for the Nusselt number and modified Blasius equation on for the friction factor.

The Nusselt number for smooth rectangular duct is given by the modified by the Dittus – Boelter equation as

$$Nu_s = 0.23 Re^{0.8} . Pr^{0.4} \left(\frac{2R_{av}}{D_h} \right)^{-0.2} \rightarrow (1)$$

The friction factor for a smooth rectangular duct is given by the modified Blasius equation as

$$f_s = 0.085 . Re^{-0.25} \rightarrow (2)$$

The comparison of the experimental and estimated values of the Nusselt number friction factor as a function of the Reynolds number is shown in fig.3 and 4. The maximum deviation observed in the Nusselt number is 7.5% and the average deviation is 5.5%. The maximum deviation in the friction factor value is 7% and the average deviations 4.66%.

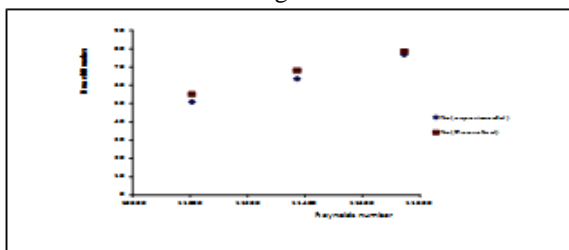


Fig.6 Comparison of experimental and predicted values of Nusselt number for smooth duct

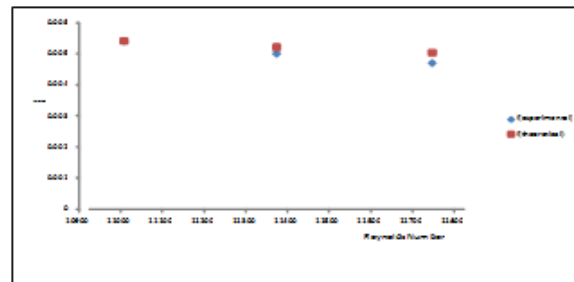


Fig.7 Comparison of experimental and predicted values of Friction factor for smooth duct

VI. RESULTS AND DISCUSSION

Heat transfer coefficient and friction factor compared roughened plate with smooth plate under similar fluid flow condition. Triangular protrusions are provided to act as roughness elements over the surface of the aluminum absorber plate to see the enhancement in heat transfer co-efficient.

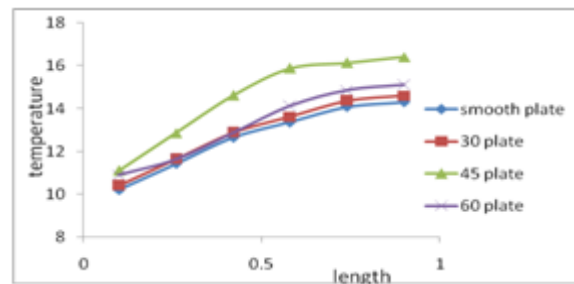


Fig. 8 Plate and Air Temperature difference Vs Length of the plate

Fig.8 shows the graphs are drawn by taking $T_{plate} - T_{air}$ on y-axis and length of the absorber plate on x-axis. From graphs it can be observed that the temperature difference is high for the plate with 45⁰ apex angle protrusion and 60⁰ plates have next highest temperature difference values. Temperature difference increases with increase in length of absorber plate. For better efficiency the length of the plate is taken as 1m. If it is more than 1m the temperature difference would not raise and if less than 1m, we may lose heat and flow.

Nusselt number vs Mass flow rate

Fig.9. Nusselt number Vs Mass flow rate increases with increase in mass flow rate. Among all the available plates smooth plate has the lowest value of Nusselt number. While the plate with 45⁰ apex angle protrusion is seen to has the highest Nusselt number at any mass flow rate of air.

Friction factor Vs Reynolds number

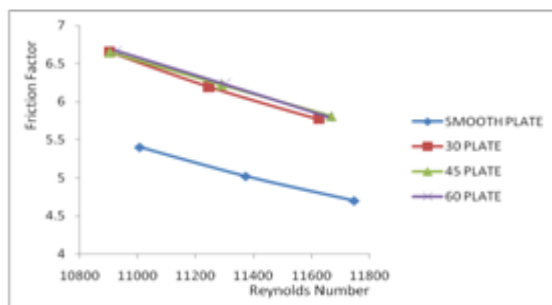


Fig. 10. Friction factor Vs Reynolds number

Fig.10 shows the variation of friction factor with Reynolds number for smooth plate and for the plates having 30°, 45° and 60° apex angle protrusions. From graph it can be seen that friction factor is highest at lower Reynolds number and decrease with an increase in Reynolds number values for all plates. The frictional factor seems to be highest for the plate with protrusions of an apex angle 60°.

Thermo-Hydraulic Performance Vs Reynolds Number

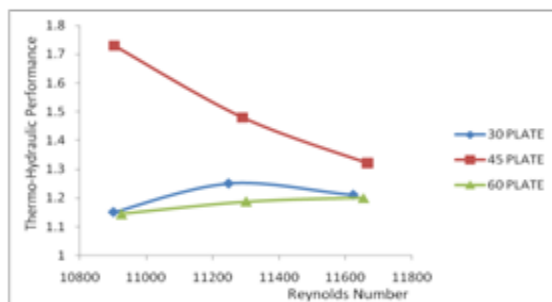


Fig. 11. Reynolds number Vs Thermo-Hydraulic Performance

Fig. 11 shows it can be seen that the Thermo hydraulic performance of the 45° plate is maximum. But it decreases with increase in Reynolds number. The Thermo hydraulic performance of the 30° plate initially increases and then decreases with the Reynolds number. The Thermo hydraulic performance of the 60° plate is the least. But it increases increase in Reynolds number.

Thermo-hydraulic performance Vs Mass flow rate

Fig. 12 shows from the graph that the thermo hydraulic performance for the plate with the 45° apex angle protrusions is highest. It is almost same for the plate with 30° and 60° apex angle protrusions. However that the thermo hydraulic performance of the plate with 45° apex angle is decreasing with increase in mass flow rate. In the case of plate with 60° apex angle protrusions however the thermo hydraulic performance is increasing, but it occurs by very smaller amount. The change of thermo hydraulic performance for the 30° is neither raising nor falling continuously.

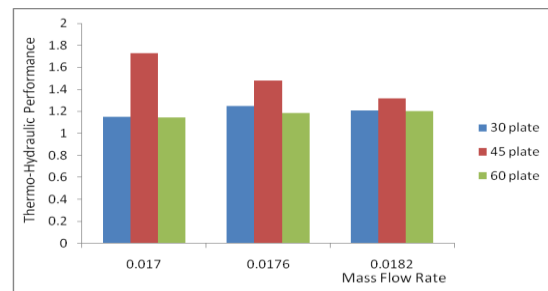


Fig. 12 Thermo-hydraulic performance for different plates

Friction factor Vs Thermo-Hydraulic Performance

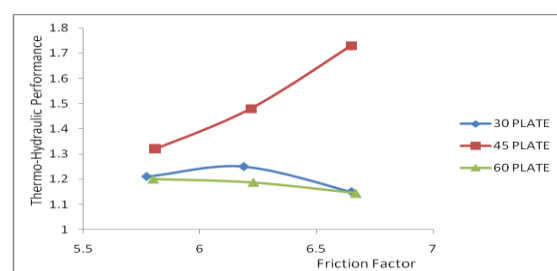


Fig. 13. Thermo-Hydraulic Performance Vs Friction factor

Fig. 13 shows that the thermo-hydraulic performance values are changing with rise in friction factor values. From the figure the friction factor values are highest for the 45° followed by the 30° and 60° respectively. It can also be observed from the graph that the rise in the friction factor values in the case of 45° apex angle protrusion implies the thermo-hydraulic performance values also rises. The values are decreasing for the 60° plate varying irregularly for the 30° plate with an increase in the friction factor.

VII. CONCLUSION

The heat transfer rate is observed maximum for the plate with 45° apex angle protrusions for any mass flow rate of air. It is concluded that 45° plates has given maximum Heat Transfer rate of 109 which is 42% higher than that of smooth plate. While the enhancement of heat transfer rate is minimum for 60° plates whole least Nusselt Number value is 81. The maximum thermo-hydraulic performance of 1.73 is observed for 45° plates while minimum value of 1.14 is observed for the 60° plate.

REFERENCES

- [1] Muluwork, K.B. Saini, J.S. and Solanki, S.C., (1998). Studies on discrete RIB roughened solar air heater, In: Proceedings of National Solar Energy Convention, Roorkee, pp. 75 -84.
- [2] Karwa R, Solanki SC and Saini JS (1999) Heat transfer coefficient and friction factor

- correlations for the transitional flow regime in rib-roughened rectangular ducts. Int. J. Heat Mass Transfer. 42(9), 1597-1615.
- [3] Gupta, D., Solanki, S.C., Saini, J.S., 1993. Heat and fluid flow in rectangular solar air heater ducts having transverse rib roughness on absorber plates. Solar Energy 51 (1), 31–37.
- [4] Verma SK, Prasad BN. Investigation for the optimal thermo hydraulic per for-manse of artificially roughened solar air heaters. Renew Energy 2000; 20:19–36.
- [5] Jaurker AR, Saini JS, Gandhi BK. Heat transfer and friction characteristics of rectangular solar air heater duct using rib-grooved artificial roughness. Solar Energy 2006; 80:895–7.
- [6] Layek A, Saini JS, Solanki SC. Second law optimization of a solar air heater having chamfered rib-groove roughness on absorber plate. Renew Energy 2007; 32:1967–80.
- [7] Karmare SV, Tikekar AN. Heat transfer and friction factor correlation for artificially roughened duct with metal grit ribs. Int J Heat Mass Transf 2007; 50:4342–51.
- [8] Saini, R.P. &Verma, J., (2008). Heat transfer and friction correlations for a duct having dimple shape artificial roughness for solar air heater, *Energy*, 33, pp. 1277-1287.
- [9] B.N. Prasad, J.S. Saini, Effect of artificial roughness on heat transfer and friction factor in a solar air heater, Solar Energy 41 (6) (1988) 555–560.
- [10] S. Eiamsa-ard, P. Promvong, Thermal characteristics of turbulent rib-grooved channel flows, International Communications of Heat and Mass Transfer 36 (2009) 705–711.
- [11] Paswan M.K. and Sharma, S.P., (2009). Thermal performance of wire-mesh roughened solar air heaters, Arab Research Institute in Science & Engineering, 1, pp. 31 – 40.
- [12] Lanjewar A., Bhagoria, J.L., Sarviya, R.M., 2011. Heat transfer and friction in solar air heater duct with W-shaped rib roughness on absorber plate. Energy 36 (7), 4531–4541.
- [13] Dhananjay Gupta, S.C. Solanki, J.S. Saini, Heat and fluid flow in rectangular solar air ducts having transverse rib roughness on absorber plates, Solar Energy 51 (1) (1993) 31–37.
- [14] S. Gupta, A. Chaube, P. Verma, Thermo-Hydraulic Performance of a Roughened Square Duct Having Inclined Ribs with a Gap on Two Opposite Walls, International Journal of Engineering Research and Development e-ISSN: 2278-067X, p-ISSN: 2278-800X, www.ijerd.com Volume 7, Issue 10 (July 2013), PP. 55-63
- [15] Gupta MK, Kaushik SC. Performance evaluation of solar air heater having expanded metal mesh and artificial roughness on absorber plate. International journal of thermal sciences 48[2009]1007-1016.
- [16] Momin AME, Saini JS, Solanki SC. Heat transfer and friction in solar air heater duct with v-shaped rib roughness on absorber plate. Int J Heat Mass Transfer 2002; 45:3383–96.
- [17] Bhagoria JL, Saini JS, Solanki SC. Heat transfer coefficient and friction factor correlations for rectangular solar air heater duct having transverse wedge shaped rib roughness on the absorber plate. Renew Energy 2002; 25:341–69.
- [18] Gupta MK, Kaushik SC. Performance evaluation of solar air heater having expanded metal mesh and artificial roughness on absorber plate. International journal of thermal sciences 48[2009]1007-1016.
- [19] Saini, R.P. &Verma, J., (2008). Heat transfer and friction correlations for a duct having dimple shape artificial roughness for solar air heater, *Energy*, 33, pp. 1277-1287.